Acetylcholinesterase inhibition studies of alkaloid components from Crinum asiaticum var. sinicum plants: In vitro assessments by molecular docking and molecular dynamics simulations

Ngo Viet Duc
Vietnam Academy of Science and Technology
Vu Thi Trang
Vietnam Academy of Science and Technology
Hoang Le Tuan Anh
Vietnam Academy of Science and Technology
Vinh Le Ba
Vietnam Academy of Science and Technology
Nguyen Viet Phong
Vietnam Academy of Science and Technology
Tran Quang Thuan
Vietnam Academy of Science and Technology
Ngo Van Hieu
Vietnam Academy of Science and Technology
Nguyen Tien Dat
Vietnam Academy of Science and Technology
Le Van Nhan
Vietnam Academy of Science and Technology
Do Thanh Tuan
Vietnam Academy of Science and Technology
Do Thi Thao
Vietnam Academy of Science and Technology
Bui Huu Tai
Vietnam Academy of Science and Technology
Le Quynh Lien
Vietnam Academy of Science and Technology
Seo Young Yang (syyang@sangji.ac.kr)
Sangji University

Research Article

Keywords: Crinum asiaticum var. sinicum, alkaloid, acetylcholine inhibitor

Posted Date: February 27th, 2023

DOI: https://doi.org/10.21203/rs.3.rs-2610193/v1

Abstract

Alkaloids are among the most important and best-known secondary metabolites as sources of new drugs from medicinal plants and marine organisms. A phytochemical investigation of whole *Crinum asiaticum* var. *sinicum* plants resulted in the isolation of seven alkaloids (**1**–**7**), including one new compound (**1**). Their structures were elucidated using NMR and HR-ESI-MS. The absolute configuration of **1** was established by ECD. A molecular docking and molecular dynamics simulation was carried out for the isolated compounds to screen for acetylcholine (AChE) inhibitory activity. The target compounds were evaluated for their inhibitory effects on AChE activity *in vitro*. The results suggest that these *C. asiaticum* alkaloids possess the ability to treat Alzheimer's disease.

Introduction

Alzheimer's disease (AD) is a brain ailment that gradually impairs memory, reasoning, and eventually the capacity to perform even the most basic tasks [1]. Numerous studies have shown that Alzheimer's patients have lower concentrations and functional levels of acetylcholine (ACh), a neurotransmitter crucial for processing memory and learning [2]. According to the World Health Organization, there are approximately 50 million people with AD currently, with cases projected to reach 152 million in 2050. Several drugs that exhibit cholinesterase inhibitory activity, such as tacrine and galantamine, have been marketed [3]. However, these medications do little to alleviate the symptoms of AD and do not repair brain damage or halt neuronal degeneration. The determination of novel therapeutic constituents in traditional herbals is a promising approach toward identifying cheaper and safe medications for the support and prevention of AD [4].

Acetylcholinesterase (EC 3.1.1.7, AChE) and butyrylcholinesterase (EC 3.1.1.8, BuChE) are two types of cholinesterases (ChEs), enzymes that hydrolyze choline esters [5, 6]. Acetylcholine (ACh) is transformed into choline and acetic acid at cholinergic synapses by the enzyme AChE [7]. One of the key foundational hypotheses for treating AD is the cholinergic theory, which postulates that a decrease in ACh levels in specific brain regions results in cognitive and memory impairment, and that preserving or restoring cholinergic functionality may alleviate these symptoms [2]. The development of cholinesterase inhibitors that block AChE may have significant therapeutic benefits for the treatment of AD [4, 8].

One of the most significant and well-recognized classes of secondary metabolites that are candidates for novel medications, from both medicinal plants and marine species, is alkaloids [9, 10]. Alkaloids are a large class of naturally occurring chemical compounds with at least one nitrogen atom that are found in both plants and marine creatures [9]. Alkaloids possess a wide range of biological effects, including anti-inflammatory, anti-cancer, antibacterial, and antioxidant activities [11, 10, 12]. Many alkaloids have been discovered and used in conventional and modern medicine, or have been the basis for the creation of novel drugs (e.g., morphine, strychnine, quinine, ephedrine, and nicotine) [13]. Morphine has been principally used as a pain medication [14]. In addition, berberine, an alkaloid derived from the *Berberis*

genus, has historically been employed in Ayurvedic, Chinese, and Middle Eastern folk medicines for its effects against a range of pathogens, including bacteria, viruses, fungi, protozoa, and helminths [15, 16].

Crinum asiaticum var. *sinicum* is used in Chinese folk medicine for treating sores, abscesses, and aching joints [17]. A methanolic extract exhibited various bioactive properties, including analgesic, anti-inflammatory, cytotoxic, and anti-cancer effects [18, 19]. Phytochemical studies showed that alkaloid components were the primary constituent, with phenolics and terpenoids as minor components [18, 20]. The alkaloid components of *C. asiaticum* extract have diverse pharmacological effects, including anti-cancer, anti-inflammatory, anti-tumor, and antibacterial properties. In our long-term research on medicinal plants [21–27], we performed a phytochemical investigation on whole *C. asiaticum* plants. This resulted in the identification of seven alkaloids, including one previously undescribed compound, bis-(−)-8-demethylmaritidine (**1**). The ability of the purified metabolites to inhibit AChE was also evaluated. The novel compound **1** showed the highest inhibitory effect, with an IC_{50} value of 80.7 ± 4.2 μM. To understand the underlying mechanisms related to AChE, molecular docking and molecular dynamics studies were performed.

Results And Discussion

Dried whole plants of *C. asiaticum* (4.0 kg) were extracted with MeOH (5 L · 3 times) at room temperature. Evaporation of the solvent under reduced pressure afforded a MeOH residue (680 g). Combined column chromatography isolation techniques of dichloromethane fractions resulted in the separation of seven compounds, including one novel alkaloid (**1**). The known metabolites were determined to be lycorine (**2**) [28], hippadine (**3**) [29], *(−)*8-demethylmaritidine (**4**) [30], pratorinine (**5**) [31], (+)-vittatine (**6**) [32], and and (-)-marithamine (**7**) [33] by analyses of their NMR spectra, as well as comparison with values in the literature.

Compound **1** was isolated as a yellow powder. The molecular formula of $C_{32}H_{36}N_2O_6$ by a chloride-attachment ion peak at *m/z* 579.2260 corresponded with $[M + Cl]^-$ (calcd 579.2262). The ^{1}H NMR of **1** displayed an aromatic proton signal at [δ_H 7.10 (1H, s, H-10)]; two olefinic groups at [δ_H 6.78 (1H, d, *J* = 10.2, H-1) and 6.04 (1H, dd, *J* = 5.4, 10.2, H-2)]; four methylene groups at [δ_H 2.08 (1H, m, H-4*α*), 1.92 (1H, m, H-4*β*), 4.39 (1H, d, *J* = 16.8, H-6*α*), 3.47 (1H, d, *J* = 16.2, H-6*β*), 2.17 (1H, m, H-11*α*), 2.35 (1H, m, H-11*β*), 3.13 (1H, m, H-12*α*), and 3.62 (1H, m, H-12*β*)]; two methine groups at [δ_H 4.34 (1H, m, H-3) and 3.73 (1H, m, H-4a)]; and one methoxy group at [δ_H 3.94 (3H, s, OCH_3)]. The ^{13}C-NMR and HSQC of **1** exhibited the signals of 16 carbon atoms, consisting of six aromatic carbons at [δ_C 122.5 (C-6), 121.2 (C-7), 143.9 (C-8), 148.4 (C-4), 106.8 (C-10), and 135.9 (C-10a)]; two olefinic carbons at [δ_C 131.1 (C-1) and 129.0 (C-2)]; four methylene carbons at [δ_C 32.5 (C-4), 60.9 (C-6), 43.6 (C-11), and 54.9 (C-12)]; two methine carbons at [δ_C 64.6 (C-3) and 63.9 (C-4a)]; and one methoxy carbon at [δ_C 56.7 (OCH_3)]. The ^{1}H and ^{13}C NMR data of **1** were similar to those of *(−)*8-demethylmaritidine (**5**), except for a difference in the chemical shift at the H-7 position [30]. The structure of **1** was deduced as a dimer of *(−)*8-demethylmaritidine (**4**) via a link

between C-7 and C-7′. Indeed, HMBC correlations were observed from H-1 to C-3, C-4a, and C-5, from H-10 to C-6a/C-8, and from H-6 to C-4a, C-7, and C-10.

The relative configuration of **1** was identified based on the agreement of NMR data with **5**, as well as support by a key NOESY experiment. The absolute configuration of **1** was identified based on circular dichroism (CD). The CD spectrum of **1** shows a positive Cotton effect signal at 290 nm (Δε + 0.61) and a negative signal at 245 nm (Δε − 0.46), allowing the α orientation of the 5,10b-ethano bridge to be determined in the structure of **1**. Additionally, the coupling constant (J = 5.4 Hz) of the protons H-2 and H-3, and the absence of a coupling constant between the allylic protons H-1 and H-3, suggest that the proton H-3 has an α-orientation. Therefore, the structure of **1** was elucidated as bis-(−)-8-demethylmaritidine.

Table 1
NMR data of compound **1**

Position	Compound 1	
	δ_C [a,b]	[a,c] δ_H (mult., *J* in Hz)
1/1'	131.1	6.78, (1H, d, *J* = 10.2, H-1)
2/2'	129.0	6.04, (1H, dd, *J* = 5.4, 10.2, H-2)
3/3'	64.6	4.34 (1H, m, H-3)
4α/4α'	32.5	2.08 (1H, m, H-4*α*)
4β/4β'		1.92 (1H, m, H-4*β*)
4a	63.9	3.73 (1H, m, H-4a)
6α/6α'	60.9	4.39 (1H, d, *J* = 16.8, H-6*α*)
6β/6β'		3.47 (1H, d, *J* = 16.2, H-6*β*)
6a/6a'	122.5	
7/7'	121.2	
8/8'	143.9	
9/9'	148.4	
10/10'	106.8	7.1 s
10a/10a'	135.9	
10b/10b'	45.9	
11α/11α'	43.6	2.17 (1H, m, H-11*α*)
11β/11β'		2.35 (1H, m, H-11*β*)
12α/12α'	54.9	3.13 (1H, m, H-12*α*)
12β/12β'		3.62 (1H, m, H-12*β*)
13/13'-OCH_3	56.7	3.94 s

[a] measured in MeOD, [b] 150 MHz, [c] 600 MHz.

Due to their distinct pharmacological or biological actions and variable structural makeup, natural materials continue to be a primary source of new drugs. Amyloid-beta plaques and neurofibrillary tangles are the two main components of AD, a neurodegenerative condition [34]. The key enzyme in the hydrolysis of one of the most well-known neurotransmitters, acetylcholine (ACh), which has been linked to the pathophysiology of AD, is the serine hydrolase acetylcholinesterase (AChE). Accordingly, enzymatic

suppression of AChE activity is a successful AD therapy method. Previously, we identified several AChE inhibitors from Korean medicinal plants, including triterpenoid saponins, flavonoids, and diarylheptanoids [4, 35]. In the current study, compound **1** showed notable inhibitory activity against AChE at a concentration of 500 μg/mL in comparison to the positive control Galantamine (90.29 ± 0.62 vs. 97.08 ± 0.48%). The novel compound **1** exhibited a greater inhibitory effect, with an IC_{50} value of 80.7 ± 4.2 μM. *In vitro* experiments showed that the dimer of *(−)*-8-demethylmaritidine had the highest inhibitory activity. Consequently, bis-(−)-8-demethylmaritidine (**1**) is a potential therapeutic inhibitor of AChE. Molecular docking and molecular dynamic simulations were thus used to investigate the underlying mechanisms of AChE.

Molecular docking is a popular technique for screens used in structure-based drug discovery [36]. The atomic-level interaction between a small molecule and a protein can be represented using molecular docking models, which enables researchers to define small molecule activity at target protein-binding sites and to learn about fundamental biochemical processes [2]. The two main processes in the docking procedure are determining the binding affinity and forecasting ligand shape, location, and orientation in these sites. The advantages of virtual screening include a limited search area, low cost, and high level of flexibility, all of which can help rapidly identify an appropriate target protein inhibitor [37]. To explore the interactions and binding of these compounds with AChE activity and to investigate the anti-AChE activity of the most active molecule, a molecular docking study was conducted. Molecular docking simulation results revealed that compound **1** had a significant effect on the active site of AChE, with a binding affinity of − 10.85 kcal/mol. Additionally, **1** bound tightly to three amino acid residues, Phe 338, Trp286, and Tyr341, in the active site of AChE via hydrogen bonds (Fig. 4A, 4B, and 4C). These molecular docking results imply that the hydroxy groups have an important role in AChE.

To determine the structural stability and fluctuations of the **1**-protein complex, after docking calculations with a period of 100 ns, a complicated molecular dynamic simulation was performed using GROMACS. The simulation trajectory's superposition of 100 ns intervals gave an impression of molecular movement (Fig. 5A). The potential energy of the complex was − 1.204×10^6 kJ/mol (Fig. 5B). The general state of the simulation and whether it has equilibrated can be shown by root-mean-square deviation (RMSD) analysis [38, 39]. A lower RMSD value indicates that the predicted structure of the protein-ligand complex is more stable, whereas a higher RMSD value suggests that the predicted structure is less stable [40, 41]. As shown in Fig. 5C, the RMSD value of AChE exhibited significant fluctuations in the 18-ns initial simulation, slowly increasing from 19 to 38 ns, and remained approximately at 3 Å from 40 ns to the end of the simulation trajectory. The RMSD of the residues in the binding site of the complex was within 1.5–2 Å (Fig. 5D). These data indicate that this complex exhibits stable molecular dynamics. Compound **1** formed an average of one to three hydrogen bonds with AChE over 10 ns (Fig. 5E) and maintained a distance of 1.8 Å from Phe338 and Tyr341 in the active site (Fig. 5F).

Conclusions

In this current study, seven alkaloids were yielded using combined open column chromatography, including one previously undescribed compound, bis-(−)-8-demethylmaritidine (**1**). Compound **1** showed the highest inhibitory effect, with an IC_{50} value of 80.7 ± 4.2 μM. The underlying mechanisms of its interaction with AChE were determined via molecular docking and molecular dynamics simulation. Taken together, *in vitro* and *in silico* data showed that compound **1** is a promising inhibitor for treatment of Alzheimer's disease that acts by inhibiting the AChE signaling pathway. Further analysis and *in vivo* studies are needed to better understand the exact mechanisms of action of this compound.

Materials And Methods

Chemicals and Reagents

The general experimental procedures were carried out similarly to those cited in previous papers with slight modifications [42, 23, 27]. Biological and chemical reagents were obtained from Sigma (Missouri, USA). The NMR spectra were measured using AVANCE III HD 600 spectrometer (Bruker, Billerica, MA, USA). Tetramethylsilane was selected as an internal reference. HR-ESI-MS data were acquired using a 6530 Accurate-Mass Q-TOF LC/MS system (Agilent, Santa Clara, CA, USA). TLC analysis was performed on Kieselgel 60 F_{254} or RP-18 F_{254s} plates. Open column chromatography was carried out using silica gel, Sephadex LH-20 and RP-C18, which were provided by Merck. By misting the isolated compounds with 10% H_2SO_4 in water and then heating for 1.5 to 2 minutes, the compounds were visualized. Solvents obtained from commercial sources were used throughout all procedures without additional purification.

Identification of plant

The whole plants of *C. asiaticum* (voucher specimen number: LS180122) were collected at Lang Son province in January 2022 and taxonomically identified by Dr. Do Thanh Tuan. The voucher specimen was deposited at the herbarium of the Center for Research and Technology Transfer, Vietnam Academy of Science and Technology.

Extraction of plants and column chromatography isolation of chemical components

Dried whole *Crinum asiaticum var. sinicum* plants (4 kg) were extracted by refluxing three times in 10 L methanol. The extracts were concentrated *in vacuo* to give a MeOH extract (680 g), which was suspended in H_2O (2.5 L) and adjusted to pH 2 with 10% HCl. The acidic aqueous phase was removed by filtration. The filtrate was loaded onto an ion-exchange resin, eluted with 20% MeOH until the eluate became colorless to yield the nonalkaloid parts, and then eluted with 2% NaOH in 65% MeOH solution (5× retention volume) to afford the crude total alkaloids. The alkaloid-containing solution was acidified to pH 5 with 10% HCl and partitioned with CH_2Cl_2 (3 × 2 L) to afford the CH_2Cl_2 extract (65 g).

The dichloromethane-soluble portion was subjected to silica gel column chromatography (CC), eluting with gradient systems of CH_2Cl_2-MeOH (100:0, 100:10, 100:30, 100:50, and 1:100, v/v). The eluted

fractions were pooled according to TLC analysis results, yielding six [five?] major fractions (NAD1–NAD5). The NAD2 fraction was separated by silica gel CC and eluted using CH_2Cl_2-MeOH-ammoniac (80:1:0.1–1:1:0.1, v/v/v) to yield three smaller subfractions, NAD2A–NAD2C. Compounds **3** (50 mg), **4** (200 mg), and **5** (8.2 mg) were obtained from fraction NAD2B (3.2 g) by separation using RP-18 (MeOH-H_2O, 1.5:1, v/v). Fraction NAD3 (2 g) was further isolated by YMC CC with acetone-H_2O (2:1, v/v) and purification over Sephadex LH-20 (MeOH-H_2O, 4:1, v/v) to yield compounds **2** (100.5 mg) and **6** (8.9 mg). Purification of NAD4 over Sephadex LH-20 (100% MeOH) using the same methodology, followed by preparative TLC and elution with CH_2Cl_2-MeOH-ammoniac (10:1:0.1, v/v/v), yielded compounds **1** (5.3 mg) and **7** (6.6 mg).

Molecular docking simulation

Molecular docking simulations were carried out using AutoDock 4.2.6 following the previous described protocol. The 3D X-ray crystallographic structure of acetylcholine (PDB ID: 1C2B) was yielded from the RCSB Protein Data Bank database (https://www.rcsb.org/) [43]. The PDB file was energy minimized and optimized by removal of water molecules and atomic clashes to get a stable confirmation.

Molecular dynamic simulation

GROMACS software version 2022.1 was used to perform the molecular dynamics simulation [44]. The topology parameters were generated from the CHARMM-GUI web server with the CHARMM36 force field. First, the simulation was minimized using the steepest descent method followed by a solvation process in the default size of cubic with the TIP3P water model. Next, the simulation was neutralized by adding counterions (Na^+ and/or Cl^-), followed by an energy minimization process for 50,000 steps. At 300 K and 1 atm, the minimal system was put into practice in an NPT ensemble. Finally, 1000 frames were generated with a recording interval of 100 ps, and the MD simulation was run for 100 ns.

Acetylcholinesterase inhibitory activity testing

Acetylcholinesterase inhibitory activities of isolated compounds was performed by the previous report [4]. The detailed procedure was described in the supplementary data.

Statistical analysis

Data are presented as the means ± SD for at least three independent experiments.

Declarations

Supplementary Materials: The following supporting information can be downloaded at: www.mdpi.com/xxx/s1, **Figure S1-S6**: 1D and 2D NMR spectra for compound **1**, as well as HR-ESI-MS data of compound **1**.

Author Contributions: All authors have their consent to participate.

Funding: This research was supported by the Ministry of Science and Technology under grand number ĐTĐL.CN-128/21, the National Research Foundation of Korea (NRF) grant funded by the Korean government (MSIT) (No. NRF-2022R1C1C1004636) and Regional Innovation Strategy (RIS) through the National Research Foundation of Korea (NRF) funded by the Ministry of Education (MOE)(2022RIS-005).

Institutional Review Board Statement: Not applicable.

Data Availability Statement: Not applicable.

Acknowledgments: Not applicable.

Conflicts of Interest: The authors declare no conflict of interest.

References

1. Larson EB, Kukull WA, Katzman RL. Cognitive impairment: dementia and Alzheimer's disease. Ann Rev Public Health. 1992;13(1):431-49.
2. Hasselmo ME. The role of acetylcholine in learning and memory. Curr Opin Neurobiol. 2006;16(6):710-5.
3. Goh CW, Aw CC, Lee JH, Chen CP, Browne ER. Pharmacokinetic and pharmacodynamic properties of cholinesterase inhibitors donepezil, tacrine, and galantamine in aged and young Lister hooded rats. Drug Metab Dispos. 2011;39(3):402-11.
4. Vinh LB, Dan G, Phong NV, Cho K, Kim YH, Yang SY. In vitro investigation of acetylcholinesterase inhibitors isolated from the fruit of *Stauntonia hexaphylla*. Chem Nat Compd. 2021;57(4):784-7.
5. Pohanka M. Determination of acetylcholinesterase and butyrylcholinesterase activity without dilution of biological samples. Chem Pap. 2015;69(8):1044-9. doi:doi:10.1515/chempap-2015-0117.
6. Pesaresi A, Lamba D, Vezenkov L, Tsekova D, Lozanov V. Kinetic and structural studies on the inhibition of acetylcholinesterase and butyrylcholinesterase by a series of multitarget-directed galantamine-peptide derivatives. Chem Biol Interact. 2022;365:110092. doi:https://doi.org/10.1016/j.cbi.2022.110092.
7. Cieslikiewicz-Bouet M, Naldi M, Bartolini M, Pérez B, Servent D, Jean L et al. Functional characterization of multifunctional ligands targeting acetylcholinesterase and alpha 7 nicotinic acetylcholine receptor. Biochem Pharmacol. 2020;177:114010. doi:https://doi.org/10.1016/j.bcp.2020.114010.
8. Belanger-Coast MG, Zhang M, Bugay V, Gutierrez RA, Gregory SR, Yu W et al. Dequalinium chloride is an antagonists of α7 nicotinic acetylcholine receptors. Eur J Pharmacol. 2022;925:175000. doi:https://doi.org/10.1016/j.ejphar.2022.175000.
9. Heinrich M, Mah J, Amirkia V. Alkaloids used as medicines: Structural phytochemistry meets biodiversity—an update and forward look. Molecules 2021 doi:10.3390/molecules26071836.

10. Souza CRM, Bezerra WP, Souto JT. Marine alkaloids with anti-inflammatory activity: Current knowledge and future perspectives. Mar Drugs. 2020;18(3):147. doi:10.3390/md18030147.
11. Li C, Wang J, Ma R, Li L, Wu W, Cai D et al. Natural-derived alkaloids exhibit great potential in the treatment of ulcerative colitis. Pharmacol Res. 2022;175:105972.
12. Macáková K, Afonso R, Saso L, Mladěnka P. The influence of alkaloids on oxidative stress and related signaling pathways. Free Radic Biol Med. 2019;134:429-44. doi:https://doi.org/10.1016/j.freeradbiomed.2019.01.026.
13. Zeng X-S, Geng W-S, Wang Z-Q, Jia J-J. Morphine addiction and oxidative stress: The potential effects of thioredoxin-1. Front Pharmacol. 2020;11:82.
14. Zhili X, Linglong C, Shuang J, Baohua Y. Comparing the analgesic effect of intravenous paracetamol with morphine on patients with renal colic pain: A meta-analysis of randomized controlled studies. Am J Emerg Med. 2020;38(7):1470-4. doi:https://doi.org/10.1016/j.ajem.2020.03.061.
15. Song D, Hao J, Fan D. Biological properties and clinical applications of berberine. Front Med. 2020;14(5):564-82.
16. Vlavcheski F, O'Neill EJ, Gagacev F, Tsiani E. Effects of berberine against pancreatitis and pancreatic cancer. Molecules. 2022;27(23):8630. doi:10.3390/molecules27238630.
17. Rahman MA, Hossain SA, Ahmed NU, Islam MS. Analgesic and anti-inflammatory effects of *Crinum asiaticum* leaf alcoholic extract in animal models. Afr J Biotechnol. 2013;12(2).
18. Mahomoodally M, Sadeer N, Suroowan S, Jugreet S, Lobine D, Rengasamy K. Ethnomedicinal, phytochemistry, toxicity and pharmacological benefits of poison bulb– *Crinum asiaticum* L. S Afr J Bot. 2021;136:16-29.
19. de Araújo RL, de Pinho CLC, Farias FO, Igarashi-Mafra L, Mafra MR. *Crinum* L. species as a potential source of alkaloids: Extraction methods and relevance for medicinal and pharmacological applications. S Afr J Bot. 2022;151:720-34. doi:https://doi.org/10.1016/j.sajb.2022.10.053.
20. Ghosal S, Shanthy A, Kumar A, Kumar Y. Palmilycorine and lycoriside: acyloxy and acylglucosyloxy alkaloids from *Crinum asiaticum*. Phytochemistry. 1985;24(11):2703-6.
21. Vinh LB, Heo M, Phong NV, Ali I, Koh YS, Kim YH et al. Bioactive compounds from Polygala tenuifolia and their inhibitory effects on lipopolysaccharide-stimulated pro-inflammatory cytokine production in bone marrow-derived dendritic cells. Plants. 2020;9(9):1240.
22. Vinh LB, Jang H-J, Phong NV, Cho K, Park SS, Kang JS et al. Isolation, structural elucidation, and insights into the anti-inflammatory effects of triterpene saponins from the leaves of *Stauntonia hexaphylla*. Bioorg Med Chem Lett. 2019;29(8):965-9.
23. Vinh LB, Jang H-J, Phong NV, Dan G, Cho KW, Kim YH et al. Bioactive triterpene glycosides from the fruit of *Stauntonia hexaphylla* and insights into the molecular mechanism of its inflammatory effects. Bioorg Med Chem Lett. 2019;29(16):2085-9.
24. Vinh LB, Jo SJ, Nguyen Viet P, Gao D, Cho KW, Koh E-J et al. The chemical constituents of ethanolic extract from *Stauntonia hexaphylla* leaves and their anti-inflammatory effects. Nat Prod Res. 2021;35(11):1852-5.

25. Vinh LB, Nguyet NTM, Ye L, Dan G, Phong NV, Anh HLT et al. Enhancement of an in vivo anti-inflammatory activity of oleanolic acid through glycosylation occurring naturally in *Stauntonia hexaphylla*. Molecules. 2020;25(16):3699.
26. Vinh LB, Park JU, Duy LX, Nguyet NTM, Yang SY, Kim YR et al. Ginsenosides from Korean red ginseng modulate T cell function via the regulation of NF-AT-mediated IL-2 production. Food Sci Biotechnol. 2019;28(1):237-42.
27. Vinh LB, Phong NV, Ali I, Dan G, Koh YS, Anh HLT et al. Identification of potential anti-inflammatory and melanoma cytotoxic compounds from *Aegiceras corniculatum*. Med Chem Res. 2020;29(11): 2020-3027.
28. Evidente A, Rosaria Cicala M, Giudicianni I, Randazzo G, Riccio R. 1H and 13C nmr analysis of lycorine and α-dihydrolycorine. Phytochemistry. 1983;22(2):581-4. doi:https://doi.org/10.1016/0031-9422(83)83051-9.
29. Ghosal S, Rao PH, Jaiswal DK, Kumar Y, Frahm AW. Alkaloids of *Crinum pratense*. Phytochemistry. 1981;20(8):2003-7. doi:https://doi.org/10.1016/0031-9422(81)84053-8.
30. Abou-Donia AH, Amer ME, Darwish FA, Kassem FF, Hammoda HM, Abdel-Kader MS et al. Two new alkaloids of the crinane series from *Pancratium sickenbergeri*. Planta Med. 2002;68(04):379-81. doi:10.1055/s-2002-26754.
31. Ali AA, El Saved HM, Abdalliah OM, Steglich W. Oxocrinine and other alkaloids from *Crinum americanum*. Phytochemistry. 1986;25(10):2399-401. doi:https://doi.org/10.1016/S0031-9422(00)81704-5.
32. Chen C-K, Lin F-H, Tseng L-H, Jiang C-L, Lee S-S. Comprehensive study of alkaloids from *Crinum asiaticum* var. *sinicum* assisted by HPLC-DAD-SPE-NMR. J Nat Prod. 2011;74(3):411-9. doi:10.1021/np100819n.
33. Pabuççuoglu V, Richomme P, Gözler T, Kivçak B, Freyer AJ, Shamma M. Four new crinine-type alkaloids from *Sternbergia* species. J Nat Prod. 1989;52(4):785-91. doi:10.1021/np50064a020.
34. Lee JC, Kim SJ, Hong S, Kim Y. Diagnosis of Alzheimer's disease utilizing amyloid and tau as fluid biomarkers. Exp Mol Med. 2019;51(5):1-10. doi:10.1038/s12276-019-0250-2.
35. Lee JS, Kim JH, Han YK, Ma JY, Kim YH, Li W et al. Cholinesterases inhibition studies of biological active compounds from the rhizomes of *Alpinia officinarum* Hance and in silico molecular dynamics. Int J Biol Macromol. 2018;120:2442-7.
36. Phong NV, Anh DTN, Chae HY, Yang SY, Kwon MJ, Min BS et al. Anti-inflammatory activity and cytotoxicity against ovarian cancer cell lines by amide alkaloids and piperic esters isolated from *Piper longum* fruits: in vitro assessments and molecular docking simulation. Bioorg Chem. 2022:106072.
37. Phong NV, Oanh VT, Yang SY, Choi JS, Min BS, Kim JA. PTP1B inhibition studies of biological active phloroglucinols from the rhizomes of *Dryopteris crassirhizoma*: Kinetic properties and molecular docking simulation. Int J Biol Macromol. 2021;188:719-28.

38. Martínez L. Automatic identification of mobile and rigid substructures in molecular dynamics simulations and fractional structural fluctuation analysis. Plos One. 2015;10(3):e0119264. doi:10.1371/journal.pone.0119264.
39. Manandhar S, Sankhe R, Priya K, Hari G, Kumar B H, Mehta CH et al. Molecular dynamics and structure-based virtual screening and identification of natural compounds as Wnt signaling modulators: possible therapeutics for Alzheimer's disease. Mol Divers. 2022;26(5):2793-811. doi:10.1007/s11030-022-10395-8.
40. Elhady SS, Abdelhameed RFA, Malatani RT, Alahdal AM, Bogari HA, Almalki AJ et al. Molecular docking and dynamics simulation study of *Hyrtios erectus* isolated scalarane sesterterpenes as potential SARS-CoV-2 dual target inhibitors. Biology. 2021;10(5):389. doi:10.3390/biology10050389.
41. Fusani L, Palmer DS, Somers DO, Wall ID. Exploring ligand stability in protein crystal structures using binding pose metadynamics. J Chem Inf Model. 2020;60(3):1528-39. doi:10.1021/acs.jcim.9b00843.
42. Cao TQ, Phong NV, Kim JH, Gao D, Anh HLT, Ngo V-D et al. Inhibitory effects of cucurbitane-Type triterpenoids from *Momordica charantia* fruit on lipopolysaccharide-stimulated pro-Inflammatory cytokine production in bone marrow-derived dendritic cells. Molecules. 2021;26(15):4444.
43. Bourne Y, Grassi J, Bougis PE, Marchot P. Conformational flexibility of the acetylcholinesterase tetramer suggested by X-ray crystallography. J Biol Chem. 1999;274(43):30370-6. doi:https://doi.org/10.1074/jbc.274.43.30370.
44. Vinh LB, Kim JH, Lee JS, Nguyet NTM, Yang SY, Ma JY et al. Soluble epoxide hydrolase inhibitory activity of phenolic glycosides from *Polygala tenuifolia* and in silico approach. Med Chem Res. 2018;27(3):726-34.

Figures

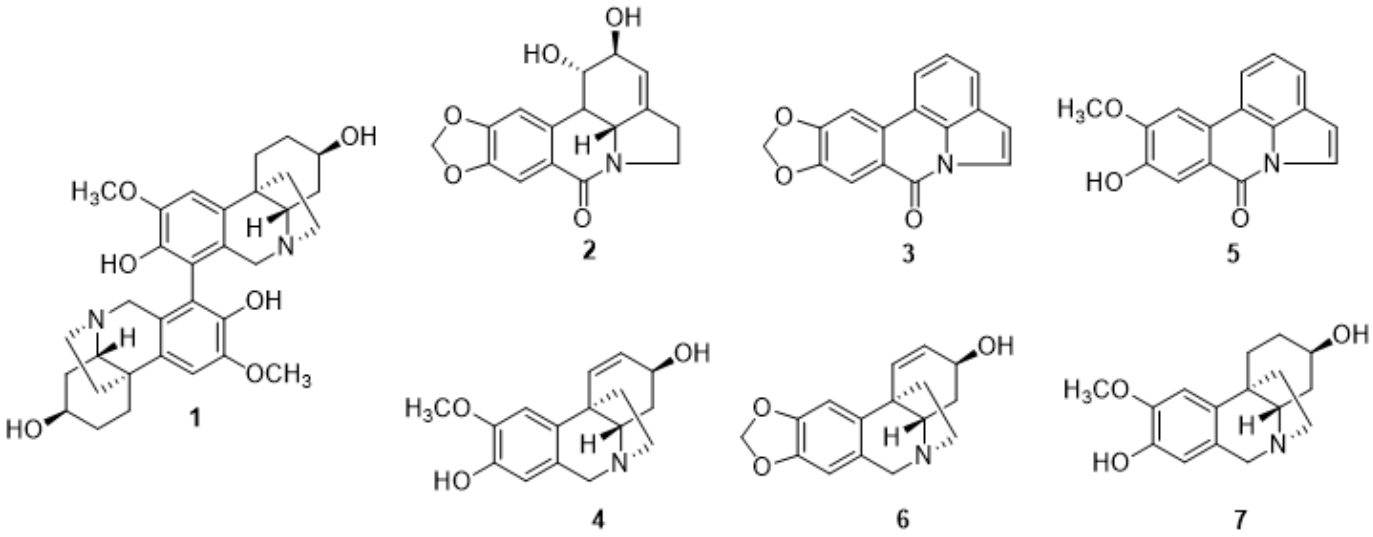

Figure 1

The structures of alkaloids (1-7) isolated from the whole plants of *C. asiaticum*

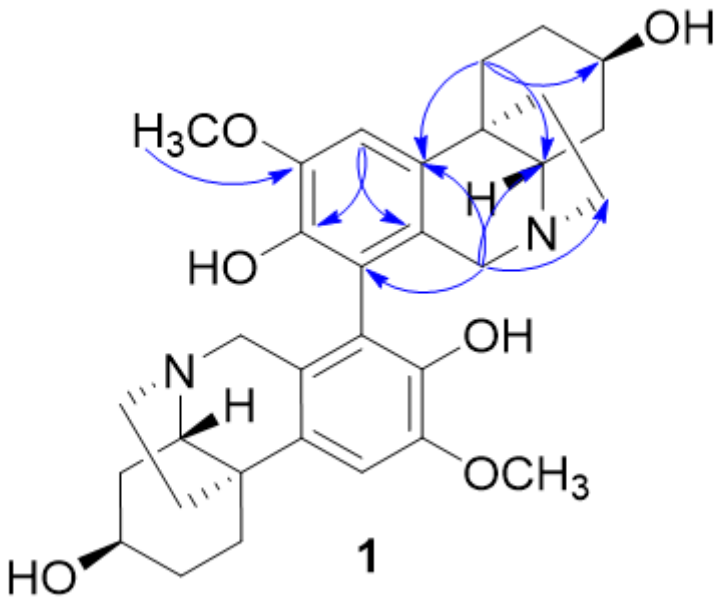

Figure 2

Significant key HMBC correlations of compound **1**

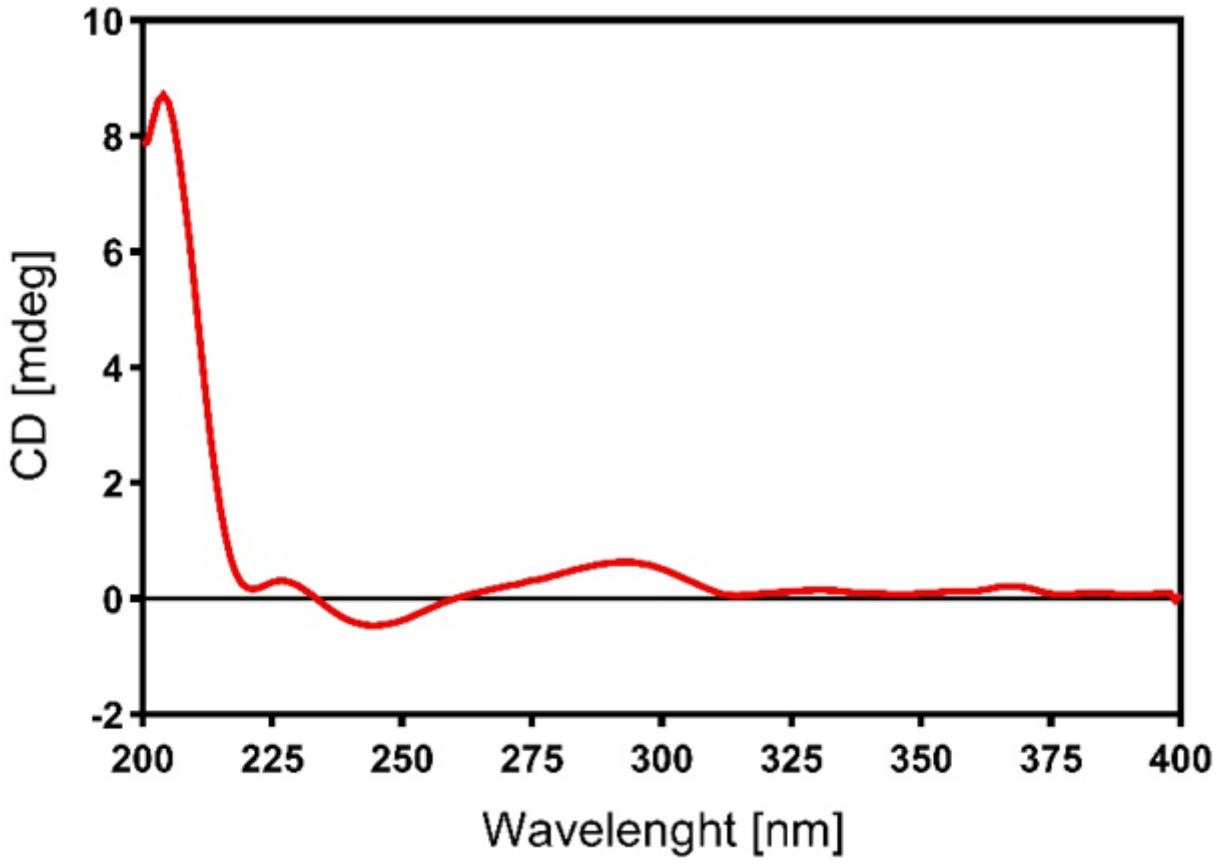

Figure 3

CD spectrum of compound **1**

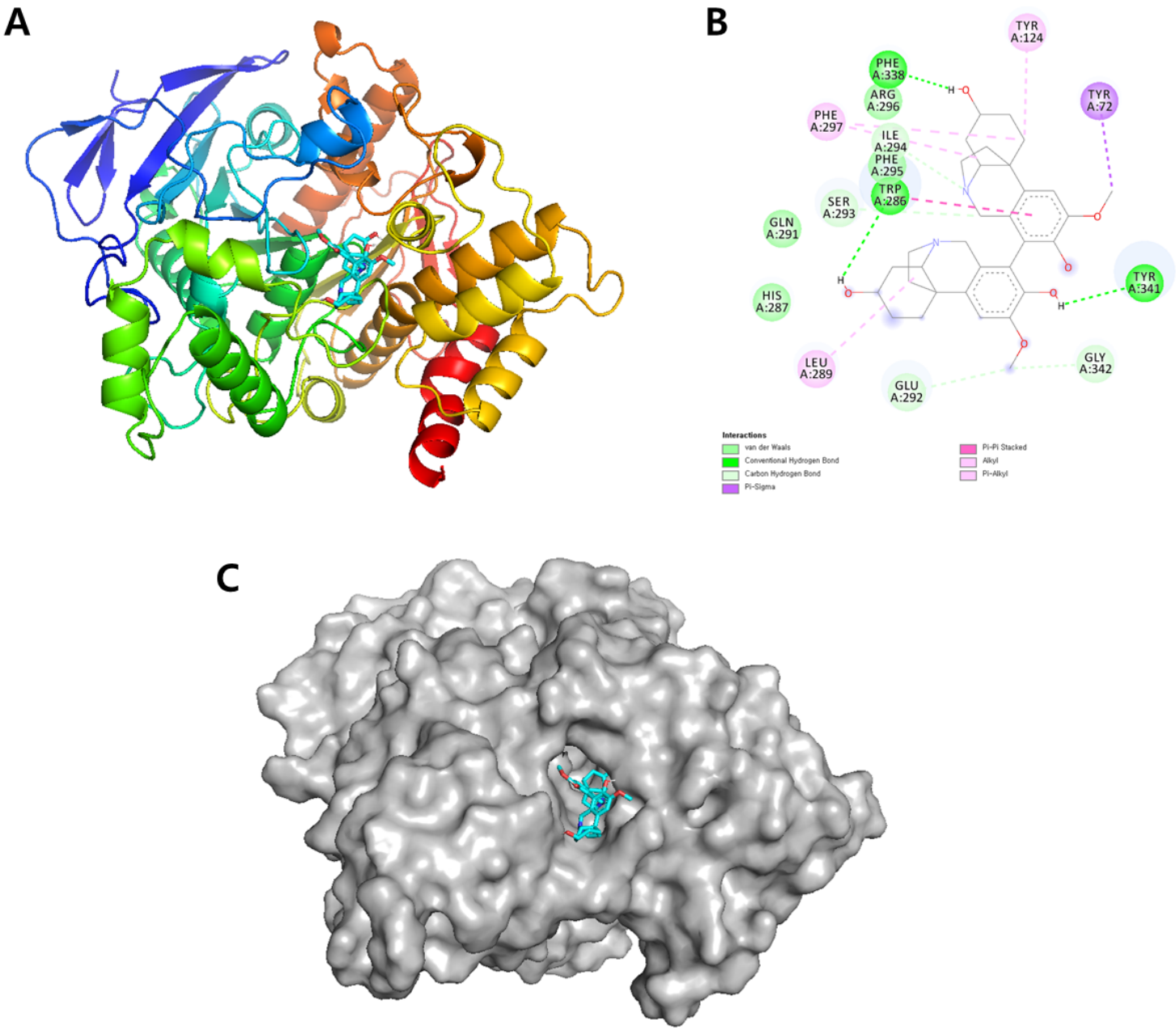

Figure 4

Molecular docking result of 1 binding to AChE protein. **(A)** 3D modeling of **1** biding within the AChE protein. (**B**) 2D interaction diagram of acetylcholine with new compound **1**. (**C**) Generation of the ligand-binding pocket.

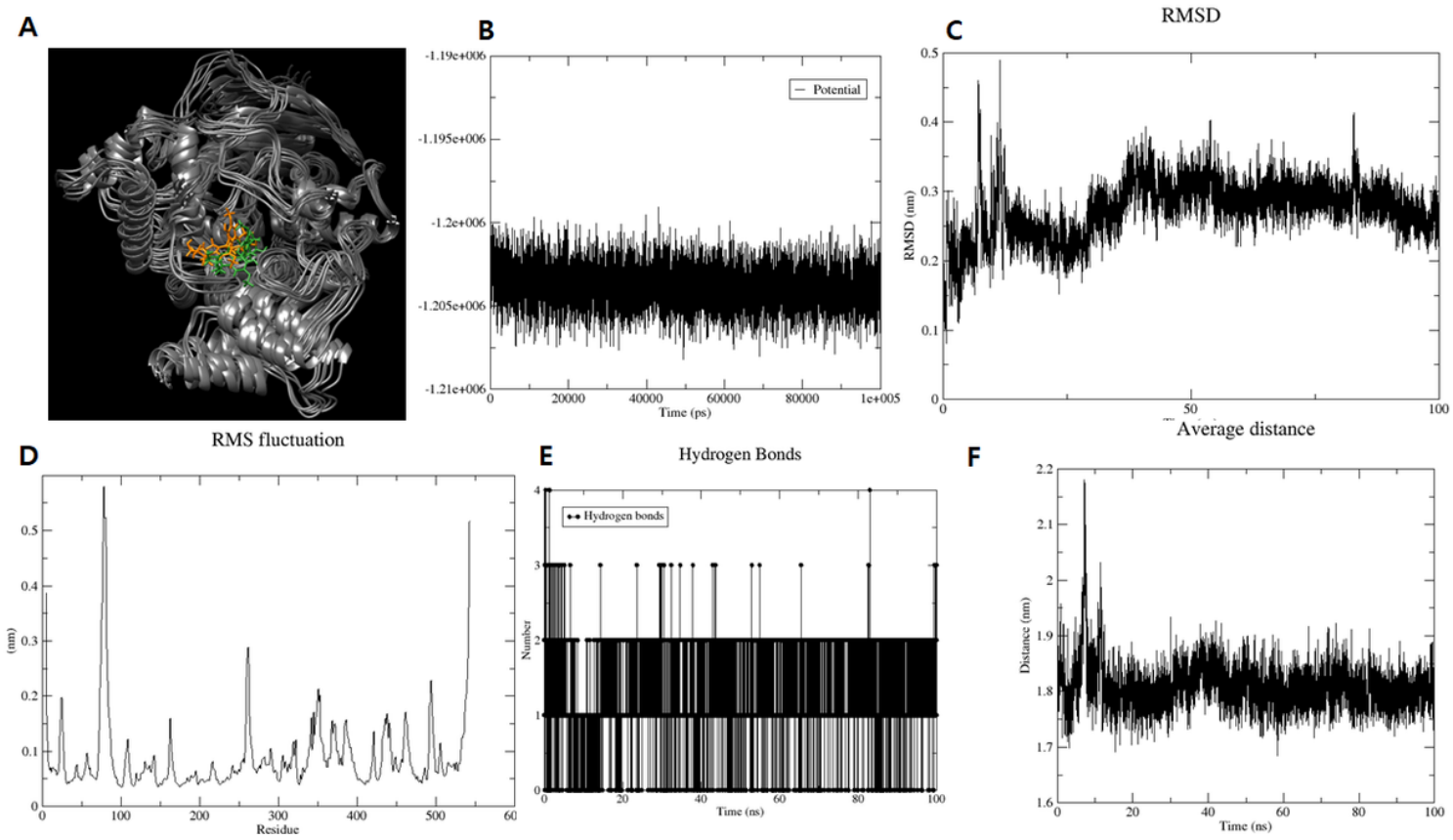

Figure 5

Superpositions of AChE with compound **1** for simulation trajectory (0 to 100 ns) (**A**). The potential energy (**B**), RMSD (**C**), RMSF (**D**), and hydrogen bonds (**E**) of the simulation calculated during 100 ns. The center of mass distance between protein and compound **1** (**F**).

Supplementary Files

This is a list of supplementary files associated with this preprint. Click to download.

- GraphicalAbstract.png
- 6.SupplementarydataCA.docx